1995

Terrigenous Fe input and biogenic sedimentation in the glacial and interglacial equatorial Pacific Ocean

R. W. Murray

M. Leinen
University of Rhode Island

D. W. Murray

A. C. Mix

Christopher W. Knowlton
University of Rhode Island, cknowlton@uri.edu

Citation/Publisher Attribution

Murray, R. W., M. Leinen, D. W. Murray, A. C. Mix, and C. W. Knowlton (1995), Terrigenous Fe input and biogenic sedimentation in the glacial and interglacial equatorial Pacific Ocean, *Global Biogeochem. Cycles*, 9(4), 667–684, doi: 10.1029/95GB02833.
Available at: https://doi.org/10.1029/95GB02833

GLOBAL BIOGEOCHEMICAL CYCLES, VOL. 9, NO. 4, PAGES 667–684, DECEMBER 1995

Terrigenous Fe input and biogenic sedimentation in the glacial and interglacial equatorial Pacific Ocean

R. W. Murray,[1] M. Leinen,[2] D. W. Murray,[3] A. C. Mix,[4], and C. W. Knowlton[2]

Abstract. Many ocean regions important to the global carbon budget, including the equatorial Pacific Ocean, have low chlorophyll concentrations despite high levels of conventional nutrients. Iron may instead be the limiting nutrient, and elevated input of terrigenous Fe during windy glacial episodes has been hypothesized to stimulate oceanic productivity through time and thus regulate the oceanic and atmospheric CO_2 balance. To test whether particulate Fe input is related to the accumulation of biogenic matter in one important low chlorophyll-high nutrient area, that is, the equatorial Pacific Ocean, we present results from a suite of sediment cores that collectively record biogenic deposition through the last six glacial-interglacial cycles (~ 600,000 years). Our data set includes new chemical data on total Fe, terrigenous, and biogenic components in three cores as well as previously published mineralogic records of eolian input to the region. Chemical, spectral, and stratigraphic analysis indicates that (1) terrigenous input to the region shows no consistent pattern of either glacial or interglacial maxima, (2) the accumulation of particulate Fe is closely related to the accumulation of terrigenous matter (linear $r^2 = 0.81 - 0.98$), (3) there are no coherent spectral relationships between Fe input and glacial periodicity (i.e., $\delta^{18}O$) in any of the orbital frequency bands, (4) the linear and cross-spectral correlations between Fe or eolian input and $CaCO_3$ concentration are most commonly the strongest observed relationships between Fe and any biogenic component, yet indicate a largely inverse pattern, with higher Fe being associated with low $CaCO_3$, (5) there is no consistent linear r^2 correlation or spectral coherence between the accumulation of Fe and that of $CaCO_3$, C_{org}, or opal. Thus in total there is no relationship between terrigenous Fe input and sedimentary sequestering of carbon. Additionally, although we cannot specifically address the potential for changes in solubility of the terrigenous fraction that may be driven by a terrigenous compositional change, the Fe/Ti ratio (which monitors first-order mineralogic changes) records only slight variations that also are linearly and spectrally unrelated to glacial periodicity, the bulk Fe flux, and the accumulation of any biogenic component. Finally, we find that the paleoceanographic flux of Fe is several order-of-magnitudes larger than modern observations of eolian Fe input, suggesting that the long-term importance of Fe input by dust storms (which deliver Fe on the order of the sedimentary burial) may be underestimated. The removal of particulate terrigenous Fe from the recently discovered source within the Equatorial Undercurrent, however, remains unquantified and may also prove significant.

Introduction

Three questions about the biogeochemical relationship between Fe and marine phytoplankton production have been highlighted for their potential importance to the oceanic and atmospheric CO_2 balance:

1. Does Fe limit modern-day production in regions like the equatorial Pacific and Southern Ocean, where low chlorophyll concentrations are associated with high levels of conventional nutrients (NO^{3-}, PO_4^{3-}, SiO_2) [*Martin et al.*, 1990, 1991; *Barber and Chavez*, 1991; *Bruland et al.*, 1991; *Morel et al.*, 1991; *Price et al.*, 1991; *Frost and Franzen*, 1992; *DiTullio et al.*, 1993; *Kolber et al.*, 1994; *Martin et al.*, 1994]?

2. Would Fe fertilization stimulate production and thus be an effective strategy to sequester atmospheric CO_2 in sedimentary calcium carbonate ($CaCO_3$) and organic carbon (C_{org}) through sedimentary burial (and thus final removal from the ocean-atmosphere system) [*Martin et al.*, 1990; *Peng and Broecker*, 1991; *Martin*, 1992; *Watson et al.*, 1994]? and

3. Did natural Fe fertilization via terrigenous input occur over glacial-interglacial timescales [e.g., *Martin*, 1990; *Berger and Wefer*, 1991]?

The equatorial Pacific plays an important role in the debate over Fe limitation of oceanic productivity because it has been specifically implicated in each of the three questions listed above and is critically important to global studies of ocean-atmosphere carbon cycling [e.g., *Murray et al.*, 1994]. As such, although models predict the Fe-fertilized consumption of conventional nutrients in the Southern Ocean is more important to the

[1]Department of Earth Sciences, Boston University, Boston, Massachusetts
[2]Graduate School of Oceanography, University of Rhode Island, Narragansett
[3]Department of Geological Sciences, Brown University, Providence, Rhode Isalnd
[4]College of Oceanic and Atmospheric Sciences, Oregon State University, Corvallis

Paper number 95GB02833.
0886-6236/95/95GB-02833$10.00

atmospheric concentration of CO_2 [*Sarmiento and Orr*, 1991], the equatorial Pacific was the location of a recently concluded experiment in which a large oceanic area was artificially fertilized with Fe and the biologic response was monitored [*Kolber et al.*, 1994; *Martin et al.*, 1994; *Watson et al.*, 1994]. Thus we focus on the equatorial Pacific Ocean to study the relationships between the input of terrigenous matter, total Fe, and biogenic sedimentation through time.

In this paper, we test the hypothesis that long-term variation in terrigenous Fe flux has been associated with sequestering of carbon in the equatorial Pacific by examining the sedimentary record of the total Fe accumulation during the last six glacial-interglacial cycles (600,000 yr = 600 kyr). We report new chemical data that result from the chemical measurement of total Fe in three cores in the vicinity of 130° - 140° W, two of which (GC51 and PC72) record Fe input for the past 600 kyr while the third (GC14) presents a shorter but higher resolution record (Figure 1; Table 1). We interpret these chemical data in the context of previously published mineralogic records of eolian input to the region, based on data from Core RC11-210 and Deep Sea Drilling Project (DSDP) Hole 503B (Table 1) [*Rea et al.*, 1986; *Chuey et al.*, 1987; *Pisias and Rea*, 1988; *Rea et al.*, 1991]. Although DSDP 503B is located well to the east of the other four cores located in the central equatorial Pacific (Figure 1), and thus in a different carbonate regime [*Snoeckx and Rea*, 1994], it is a particularly well-studied core in terms of the biogenic and eolian components (Table 1), and so it is appropriate to consider here. As we discuss below, our results address the first-order issue of the biogenic response to the total Fe input to the system, not the amount of reactive Fe. We will also address, however, the glacial-interglacial timing and extent of potential variations in reactive Fe input, and provide quantitative constraints on such potential variation.

Biogenic Production: The Sedimentary Record

Considering the capability of the sedimentary paleochemical record to provide insight into the three biogeochemical questions

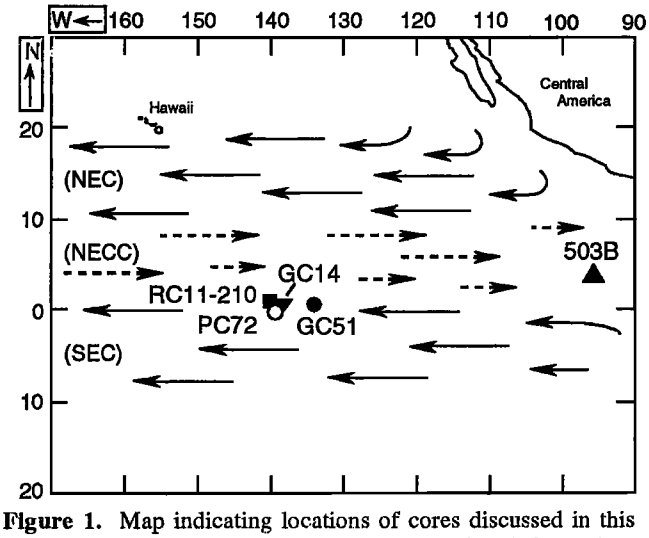

Figure 1. Map indicating locations of cores discussed in this study. See Table 1 for complete geographic information. Representative positions of surface ocean currents schematically shown as follows: NEC, North equatorial Current; NECC, North equatorial Countercurrent; SEC, South equatorial Current.

highlighted above, there are several critical issues that first must be addressed. We are unable to address question 1 through investigation of the paleochemical record because even the youngest sampled sediment in the region provides only a cumulative average signal of deposition over the past ~ 500 yr [e.g., *Murray and Leinen*, 1993; and references therein]. There is a rich literature that more appropriately addresses the topic of Fe limitation in the present-day equatorial Pacific (as cited above).

To investigate the second question quantitatively requires an understanding of the causes of the biogenic sedimentary cycles in the equatorial Pacific. The literature provides much discussion of whether Quaternary $CaCO_3$ and C_{org} maxima throughout the equatorial Pacific predominantly reflect variations in productivity [e.g., *Arrhenius*, 1952; *Pedersen*, 1983; *Lyle et al.*, 1988, 1992; *Archer*, 1991; *Pedersen et al.*, 1988, 1991; *Murray et al.*, 1993; *Herguera and Berger*, 1994] or dissolution intensity [e.g., *Berger*, 1973; *Emerson*, 1985; *Farrell and Prell*, 1991]. Indeed, although the debate is often posed in a mutually exclusive framework (i.e., production or dissolution), it is more appropriate to consider the linkage between the two processes: As synthesized by *Berger* [1992], it is the large-scale glacial-interglacial changes in productivity that may also be responsible for varying dissolution intensity. While it is beyond the scope of this paper to settle or debate this issue, we believe that the biogenic cycles we discuss predominantly reflect productivity variations. There are many lines of evidence to support this, including the broadly similar patterns of $CaCO_3$, C_{org}, and opal accumulation [e.g., *Lyle et al.*, 1988; *Rea et al.*, 1991] (each responding to different dissolution mechanisms; e.g., *Martin et al.*, [1991]), modeling considerations [e.g., *Archer*, 1991], a variety of trace metal proxies such as Ba, sedimentary I, scavenged Al, and redox sensitive metals [e.g., *Pederson*, 1983; *Pederson et al.*, 1988; *Dymond et al.*, 1992; *Murray et al.*, 1993; *R. W. Murray and M. Leinen*, unpublished data, 1995], faunal abundances [e.g., *Pederson et al.*, 1988; *Herguera and Berger*, 1991], as well as others. Most importantly, recall that question 2 concerns the relationship between Fe input and sequestration of atmospheric CO_2 through final sedimentary burial. Thus variations in dissolution that are superimposed upon the larger productivity signal [e.g., *Wei et al.*, 1994] will not compromise the sedimentary paleochemical record's capability to accurately document temporal changes in final carbon sequestration and terrigenous Fe input.

Building on this discussion, the final question, which addresses the most important issue of this paper, will be addressed below by comparison of the terrigenous Fe input through time. By monitoring the input of terrigenous material, the input of Fe, and the accumulation of the biogenic components, we will examine the relationship between the potential for Fe fertilization and the biogenic response.

Sources of Eolian, Terrigenous, and Particulate Fe

The Fe hypothesis of phytoplankton limitation in the equatorial Pacific was originally phrased in the context of the Fe being delivered via eolian input [e.g., *Martin*, 1990; *Martin et al.*, 1994]. Recently, however, it was discovered that the Equatorial Undercurrent (EUC) carries a substantial dissolved and particulate load of Fe to the central equatorial Pacific, and that

Table 1. Core Locations and Data Type

Core	Latitude, deg North	Longitude, deg West	Depth, m	Data Type	Data Source
WEC8803B-GC51	1.3	133.6	4410	Fe, Ti, $CaCO_3$, C_{org}, opal	This work, and *Murray et al.* [1993]
WEC8402A-GC14	0.95	139	4287	Fe, Ti, $CaCO_3$, C_{org}, opal	This work, and *Murray* [1987]
TT013-PC72	0.1	139.4	4298	Fe, Ti, $CaCO_3$	This work
RC11-210	1.8	140	4420	Eolian, $CaCO_3$, C_{org}, opal	*Chuey et al.* [1987] *Pisias and Rea* [1988] *Rea et al.* [1991]
DSDP 503B	4.0	95.6	3672	Eolian, $CaCO_3$, C_{org}, opal	*Rea et al.* [1986]

this EUC input is a far more significant source to the euphotic zone than eolian input [*Gordon et al.*, 1995]. Chemical analyses of this EUC particulate matter suggest that it is similar in composition to upper continental crust [*Gordon et al.*, 1995], and thus at this point we cannot distinguish in the sediment between particulate matter advected in the EUC and eolian particulate matter. Because of this, we refer to the total Fe in the sediment in the cores which we chemically analyzed as "terrigenous" (i.e., indistinguishable between advected and eolian sources). For RC11-210 and DSDP 503, however, the operationally defined eolian fraction was analyzed by previous workers (discussed below), and we indeed refer to this fraction as "eolian". The Fe analyses measure variation in the amount of total Fe supplied to the system via the combined sources of eolian input and the EUC, and we are thus examining in the sedimentary record the Fe fertilization hypothesis in the context of the relationship between the total Fe input and biogenic sedimentary response.

Analytical Methodology and Stratigraphy

Complete core and geographic information is provided in Table 1, as is a summary of the available data discussed in this paper. Calcium carbonate in gravity core WEC8803B-GC51 (subsequently abbreviated as "GC51") and piston core TT013-PC72 (abbreviated as "PC72") was determined by standard coulometric techniques, as was C_{org} in GC51 (see *Murray et al.* [1993] for determinations of precision and accuracy). Opal in GC51 was determined using a normative calculation that was calibrated to opal measured by a timed-dissolution technique on similar samples from the equatorial region [*Murray and Leinen*, 1993]. Biogenic components in WEC8402A-GC14 (abbreviated as "GC14") were determined as described in *Murray* [1987]. Data for the biogenic components in RC11-210 and DSDP 503B (abbreviated as "503B") were taken from the literature [*Rea et al.*, 1986; *Chuey et al.*, 1987; *Pisias and Rea*, 1988; *Rea et al.*, 1991].

For GC51, total Fe and Ti were determined by Xray fluorescence spectrometry (XRF) (XRay Assay Laboratories, Toronto, Canada); precision, determined by blind analysis of ~ 10 replicate powders submitted over three different analytical runs several months apart, is 7% of the measured value for Fe and 2% of the measured value for Ti. Accuracy was assessed by blind analysis of reference sediment NBS-1C (argillaceous limestone, Fe = 0.38 wt. %; Ti = 0.04 wt. %); values agree within precision. To verify Fe data in GC51, 21 samples selected to represent the entire Fe concentration range were also analyzed by inductively coupled plasma-emission spectrometry (ICP-ES) at Boston University, using sample preparation methods described by *Murray and Leinen* [1993]. Agreement between XRF and ICP-ES data was excellent even for the lowest Fe concentrations, and because the ICP-ES data are preferred for reasons of quality control the original XRF data were slightly corrected by a linear regression generated from the comparative data ($r^2 = 0.984$). These corrections do not affect the temporal pattern of Fe abundance or accumulation in any way, and the dual measurements serve to verify and confirm the analytical results. Owing to the extremely high $CaCO_3$ concentrations in some samples (up to 91 wt. %), some Ti values are below the XRF detection limit. For PC72, Fe and Ti were determined by ICP-ES at Boston University. Precision was assessed by repeated preparation and analysis of sediment from the 432- to 433-cm interval of PC72, and is 4% of the measured value for both Fe and Ti. Accuracy was assessed by analysis of reference sediment NBS-1C (described above), values agree within precision. Because the amounts of Fe and Ti in NBS-1C are somewhat greater than are found in equatorial Pacific samples, however, we also analyzed an aliquot of NBS-1C that had been diluted as a powder by ultrapure $CaCO_3$ powder (ULTREX, J. T. Baker, Inc.) to Fe and Ti concentrations (Fe ~ 300 ppm, Ti ~ 30 ppm) more representative of or lower than those found naturally. The analyzed concentrations of both Fe and Ti in this modified reference, as well as the Fe/Ti ratio, also agreed within precision to the expected values. For GC14, Fe and Ti were determined using a wavelength dispersive Philips PW1600 simultaneous XRF spectrometer at Oregon State University [*Murray*, 1987]. Values presented here have been slightly adjusted from the original data in *Murray* [1987], based on comparative atomic absorption spectrometry (AA) analyses of a suite of samples from GC14 and a nearby box core. Although the trends are similar,

XRF values were subsequently linearly corrected to the preferred AA results; again, these corrections do not affect the temporal pattern of Fe abundance or accumulation in any way and the dual measurements serve to verify and confirm the analytical results. Precision of the GC14 analyses remains better than 3% and accuracy is better than 7% of the measured value.

The age model for GC51 ties together the $\delta^{18}O$-based age model using *Globorotalia tumida* from 0 to 412 kyr [*LaMontagne*, 1993] and the carbonate-based age model from 412 to 619 kyr [*Murray et al.*, 1993] that is based on correlation of $CaCO_3$ concentration in GC51 to that in RC11-210 which is in turn isotopically calibrated to the SPECMAP stack [*Pisias and Rea*, 1988]. The age model for GC14 is based on a correlation to the SPECMAP stack [*Imbrie et al.*, 1984] of the $\delta^{18}O$ record measured on *G. tumida* using the signal correlation technique of *Martinson et al.* [1982] and eight coefficients to define the mapping function. Accumulation rates for GC14 presented here are slightly different from those presented graphically by *Lyle et al.* [1988], due to small revisions of the age model. The age model for PC72 was determined by $\delta^{18}O$ analysis of *Cibicides wuellerstorfi* and correlation to the SPECMAP stack [*Imbrie et al.*, 1984]. The age models for RC11-210 and 503B are taken from the literature [*Rea et al., 1986; Pisias and Rea, 1988*]. Only the 0 to 600 kyr portion of the published record from RC11-210 is reproduced here because it is only this interval that we can compare to the 0 to 600 kyr records of GC51 and PC72. As will be shown below, slight differences in the age models between the various cores discussed here will not affect the main points of this paper. We instead emphasize variations within each core and further note that these variations are internally consistent between the cores.

Accumulation rates were calculated using the standard protocol of the accumulation rate of a given element (or component) equaling the product of linear sedimentation rate (derived from the age model), dry bulk density, and concentration of the element or component in question. For GC51 and PC72, dry bulk density was calculated from a relationship between $CaCO_3$ and dry bulk density specific to this region [*Murray and Leinen*, 1993]. For GC14, dry bulk density was determined using methods described by *Murray* [1987]. The accumulation of the biogenic and eolian components in RC11-210 and 503B are taken from *Rea et al.* [1986], *Chuey et al.* [1987], and *Pisias and Rea* [1988], in which the operationally defined eolian component was determined by a series of chemical extractions. Eolian accumulation rates in RC11-210 for samples younger than 50 kyr are not presented because they are referred to by the original authors as "anomalous"; there also is an ash layer at 75 kyr [*Chuey et al.*, 1987]. In 503B, the eolian and opal accumulation rates were measured on slightly different intervals than were the accumulations of $CaCO_3$ and C_{org}. For purposes of calculating correlation coefficients (see below), the accumulations of eolian and opal were linearly interpolated onto the depths for which $CaCO_3$ and C_{org} were measured.

Spectral analyses of the cores for which we have chemical data was performed using standard menu-driven software from Brown University that is based on the Blackman-Tukey method [*Jenkins and Watts*, 1968]. For GC51, spectral analyses were performed only on the portion of the core with ages that are isotopically defined (0 to 412 kyr). Interpretation of the 100 kyr period in GC14 (a 240 kyr record) must be made with caution because only two 100 kyr cycles are recorded.

Results

Data for GC51, GC14, and PC72 are given in the appendices (Tables A1 - A3). Linear correlation coefficients (r^2) between the accumulation of the biogenic components, the accumulation of the respective eolian component, the Fe/Ti ratio (g/g), and the concentration of $CaCO_3$ (wt. %) are given in Table 2. Results of cross-spectral analyses are given in Table 3. Downcore profiles of the various components for each core are presented in Figures 2 - 6. The concentration of $CaCO_3$ is plotted only for the cores for which the new Fe data is given (GC51, GC14, and PC72); similarly, spectral analyses were only performed on these cores.

Downcore profiles of $CaCO_3$ concentration and accumulation in all cores display the well-known increases and decreases that broadly follow glacial-interglacial cyclicity (as cited above). In GC51, GC14, and PC72, the accumulation of Ti, which we use to track terrigenous input [*Taylor and McLennan*, 1985; *Murray et al.*, 1993], records maxima during both glacial and interglacial periods, with no consistent pattern. In all cores, the accumulation of Fe closely follows that of the terrigenous component, as measured by Ti (Tables 2 and 3). Most significantly, in these cores the accumulation of Fe is not related to the accumulation of $CaCO_3$, C_{org}, or opal, neither in terms of the linear r^2 values (Table 2) nor in terms of spectral coherence (Table 3). In four of the five cores, the strongest linear r^2 correlation between Fe or terrigenous accumulation and any biogenic variable is with $CaCO_3$ wt. %, and this correlation is negative. (The relatively strong r^2 between Fe and opal accumulation in GC51 results essentially solely from the paired maximum at ~ 330 kyr.) In the one core for which the correlation is not negative (RC11-210), the correlation between eolian input and $CaCO_3$ wt. % is exactly zero and the correlation between eolian input and the accumulation of $CaCO_3$, C_{org}, and opal also are essentially zero (respectively, 0.01, 0.02, and 0.04; Table 2). Spectral analyses confirm the lack of consistent relationship between the accumulation of Fe and the accumulation of any biogenic component at any orbital frequency, as well as the much stronger and essentially inversely related (~ 180° out-of-phase) relationship between Fe accumulation and $CaCO_3$ abundance (Table 3).

In GC51 and PC72, the Fe/Ti ratio records a long-term decrease from 600 kyr to ~ 350 kyr, after which it either slightly increases or maintains a relatively constant median value to modern-day levels (Figures 2 and 4). There are also higher frequency variations superimposed on these long-term trends, such as found in GC14 (Figure 3). Neither the long-term trend nor the short-term variability in Fe/Ti is related to glacial periodicity, nor are they significantly related to the accumulation of any biogenic component (Tables 2 and 3).

In RC11-210, the accumulation of the eolian component records both glacial and interglacial maxima (Figure 5). In 503B, eolian accumulation appears to be predominantly interglacial (Figure 6). In both cores, eolian accumulation is unrelated to the accumulation of any of the biogenic components.

Discussion

For the following reasons, we interpret the Fe profiles in GC51, GC14, and PC72 as records of the terrigenous input of Fe

Table 2. Linear Correlation Coefficients Between Fe, Ti, and Biogenic Accumulation, as well as Fe/Ti and $CaCO_3$ Abundance

	Fe	Ti	$CaCO_3$	C_{org}	Opal	Fe/Ti	$CaCO_3$,%	Eolian
				GC51 (0 - 600 kyr)				
Fe	1.00							
Ti	0.93	1.00						
$CaCO_3$	0.09	0.05	1.00					
C_{org}	0.16	0.14	0.24	1.00				
Opal	0.53	0.50	0.46	0.41	1.00			
Fe/Ti	- 0.08	- 0.20	0.00	- 0.03	- 0.06	1.00		
$CaCO_3$ (%)	- 0.17	- 0.24	0.30	0.00	0.00	0.26	1.00	
				GC14 (0 - 240 kyr)				
Fe	1.00							
Ti	0.81	1.00						
$CaCO_3$	- 0.01	0.04	1.00					
C_{org}	0.00	0.03	0.48	1.00				
Opal	- 0.07	- 0.01	0.04	0.18	1.00			
Fe/Ti	0.23	0.00	- 0.27	- 0.17	- 0.14	1.00		
$CaCO_3$ (%)	- 0.11	0.00	0.73	0.30	0.00	- 0.26	1.00	
				PC72 (0 - 600 kyr)				
Fe	1.00							
Ti	0.97	1.00						
$CaCO_3$	- 0.01	- 0.03	1.00					
Fe/Ti	- 0.05	- 0.15	0.12			1.00		
$CaCO_3$ (%)	- 0.46	- 0.52	0.35	0.16			1.00	
				RC11-210 (0 - 600 kyr)				
Eolian								1.00
$CaCO_3$			1.00					0.01
C_{org}			0.54	1.00				0.02
Opal			0.05	0.05	1.00			0.04
$CaCO_3$ (%)			0.55	0.20	- 0.03		1.00	0.00
				DSDP 503B (0 - 420 kyr)				
Eolian								1.00
$CaCO_3$			1.00					- 0.15
C_{org}			0.00	1.00				0.15
Opal			- 0.45	0.21	1.00			0.37
$CaCO_3$ (%)			0.79	- 0.10	- 0.72		1.00	- 0.39

Linear correlation coefficients are r^2. Missing values are for data not gathered for that particular core. $CaCO_3$ % is $CaCO_3$ abundance.

to the central equatorial Pacific: (1) This region is not affected by the largescale hydrothermal inputs that are located well to the east [*Leinen and Stakes,* 1979; *Dymond,* 1981; *Murray and Leinen,* 1993]; (2) although the Fe/Ti ratios in these cores (ranging from ~ 10 to 25) are often somewhat greater than that of average pelagic clay (= 14) [*Taylor and McLennan,* 1985] and Mesozoic/Cenozoic andesite (= 11) [*Condie,* 1993] (and thus could be interpreted as reflecting variation in the abundance of diagenetic oxides), iron oxides, however, are themselves known to be common components of eolian dust [*Duce and Tindale,* 1991; and references therein]; (3) the fact that the Fe and Ti accumulation profiles record identical downcore patterns in each of the three cores indicates that the Fe and Ti share a primary and common terrigenous source; and (4) Fe accumulation varies by up to a factor of 4, which is greater than can be explained by the maximum potential variation (between 30 and 45%; *Murray* [1987]) in the diagenetic and eolian oxide component, indicating that oxides are not the primary Fe-bearing phase in these sediments. Thus we conclude that our measurements of total Fe reflects terrigenous Fe in these sediments.

Glacial and Interglacial Input of Fe

The temporal patterns of Fe input in these cores do not support the hypothesis that long-term variation in total Fe input controls glacial-interglacial biogenic cyclicity [*Martin,* 1990; *Berger and Wefer,* 1991]. First, the terrigenous and eolian accumulation patterns (based on Ti in GC14, GC51, and PC72, and the eolian measurements in RC11-210 and 503B) show no consistent increase during glacial episodes. Second, linear and spectral analysis show that there is no evidence that $CaCO_3$, C_{org}, or opal accumulation was related to the flux of Fe during the past six glacial-interglacial cycles. Third, the linear r^2 and spectral correlations between Fe or eolian input and $CaCO_3$ concentration is either negative or zero (for the r^2) or essentially 180° out-of-phase (for the cross-spectral analysis, and only where there is any relationship at all). Thus there is no evidence that the input of Fe influenced the final sedimentary sequestering of biogenically produced carbon in the equatorial Pacific.

Comparing these chemical records to the mineralogic studies of eolian accumulation in RC11-210 and 503B confirms the lack

Table 3. Results of Cross-Spectral Analysis, Cores GC14, GC51, PC72

Variables	Core	Phase Difference ± Phase Error / Coherency ^{2} 100 kyr	41 kyr	23 kyr
Fe acc. / $\delta^{18}O$	GC14	- 261 ± 12 / 0.84		
	GC51		97 ± 20 / 0.60	
	PC72	92 ± 10 / 0.81		
Fe acc. / Carb. %	GC14	131 ± 14 / 0.81		
	GC51		177 ± 17 / 0.69	169 ± 18 / 0.65
	PC72	160 ± 12 / 0.76	- 178 ± 13 / 0.71	- 164 ± 11 / 0.79
Fe acc. / Carb. acc.	GC14	122 ± 17 / 0.72		
	GC51			
	PC72	119 ± 21 / 0.50		
Fe acc. / C_{org} acc.	GC14			
	GC51			
Fe acc. / Opal acc.	GC14	192 ± 25 / 0.54		
	GC51			
Fe acc. / Ti acc.	GC14	5 ± 4 / 0.98	17 ± 7 / 0.95	21 ± 11 / 0.86
	PC72	1 ± 2 / 0.99	1 ± 2 / 0.99	5 ± 3 / 0.98
Fe/Ti / $\delta^{18}O$	GC14	116 ± 13 / 0.84		
	GC51			40 ± 19 / 0.64
	PC72			

Cross-spectral analysis based on the Blackman-Tukey method [*Jenkins and Watts*, 1968]. Positive phase angles indicate the first variable leads the second. No phase angle is given if records are not coherent at the 80% confidence level, or if one variable shows no increase in variance at the period of interest. Values of coherency^2 at 80% confidence are as follows: Core GC14 = 0.52; GC51 = 0.42; PC72 = 0.29, with respective bandwidths of 0.0133, 0.0095, and 0.0095 and lags of 25, 35, and 35. All records interpolated at Δt = 2 kyr with cross-spectral analysis performed at Δt = 4 kyr. For Core GC51, only the 0 - 412 ky was analyzed (the portion of the core for which ages are isotopically defined; see text); PC72 was analyzed from 0 - 600 kyr. Note that GC14 records only 240 kyr of deposition and thus the 100 kyr period is defined only by two cycles. Ti accumulation not included for GC51 due to many values being below XRF detection limit (Table A1).

of relationship between eolian input and biogenic accumulation. In RC11-210, eolian accumulation exhibits both interglacial and glacial maxima and does not correspond to the accumulation of any biogenic component. Similarly, in the shorter record at DSDP 503B, eolian accumulation does not correspond to either $CaCO_3$ accumulation maxima or minima.

In addition to addressing the Fe fertilization hypothesis, these collected chemical and mineralogic data further document that the equatorial Pacific does not exhibit the same "glacially dusty" patterns found in Antarctic ice [*Petit et al.*, 1990] and northwest Pacific sediment [*Hovan et al.*, 1991]. This discrepancy emphasizes the importance of the temporal and spatial patchiness of terrigenous input to the surface and near-surface ocean. Indeed, as noted by *Boyle* [1983] in a study of a core located in the far eastern equatorial Pacific, the collected data sets indicate that such inputs not only respond to global aridity and wind strength, but to other factors as well.

Solubility Variation of the Terrigenous Component?

The sedimentary Fe data cannot resolve differences in the soluble fraction of terrigenous input (~10 % of the total Fe input) [*Duce and Tindale*, 1991] through time and we therefore cannot explicitly rule out potential changes in Fe solubilization (and thus bioavailability of dissolved Fe) that may result from variation in weathering or mineralogy of the terrigenous source over the glacial-interglacial timescale. Any hypothesis of Fe fertilization that requires temporal variation of Fe solubility, however, must invoke the solubility being unrelated to both Fe input and the total terrigenous input. Indeed, our data indicate that there is no increase in biogenic burial during those time periods where the terrigenous Fe input in fact increases by up to a factor of 5 (Figures 2 - 4). Thus if an Fe fertilized system were operating, the solubility of the terrigenous fraction would have to decrease during those periods of high particulate input. Recall, however, that neither the long-term decrease nor the higher frequency variations in Fe/Ti in GC51, GC14, or PC72 correspond to glacial-interglacial cyclicity in biogenic burial, which implies that neither the Fe source terrain nor the solubility of the Fe component is varying in concert with biogenic production. This variation in Fe/Ti is nonetheless intriguing; future studies of the terrigenous sediment fraction and potential source terrains should address this variation in order to constrain these observations.

Terrigenous Input of Fe to the Equatorial Pacific

The results of this study also address the input budget of Fe to equatorial Pacific waters. Modern estimates of the total average

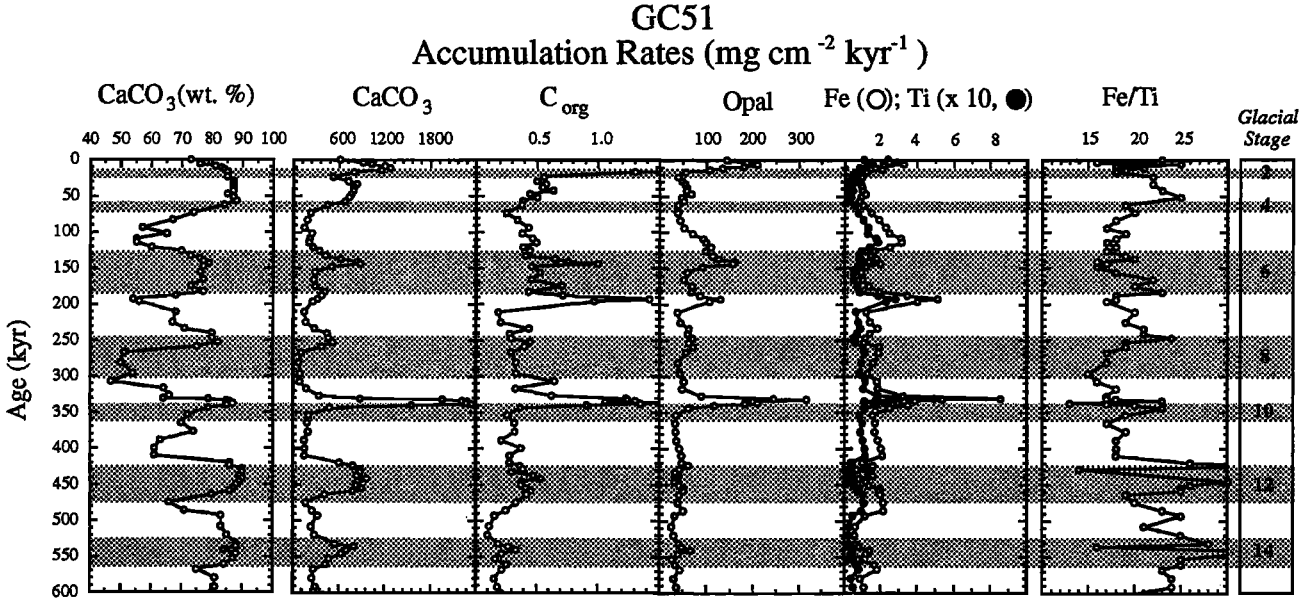

Figure 2. Downcore age profiles of the concentration of $CaCO_3$ (wt. %) in GC51 (with numbered and shaded isotopic glacial stages from *Imbrie et al.* [1984]), the accumulation rates of $CaCO_3$, C_{org}, opal, Fe, and Ti (x 10), as well as the age profile of Fe/Ti. Missing values in Ti accumulation and Fe/Ti reflect Ti concentrations below analytical detection limit (see text).

eolian flux of Fe to the ocean in the equatorial Pacific are on the order of 0.1 mg cm^{-2} kyr^{-1} [*Duce and Tindale*, 1991]. This value is at least an order of magnitude smaller than that recorded in sediment over the longer timescale (Figures 2 - 4) as well as substantially smaller than values calculated from the eolian accumulation record at RC11-210 and 503B (based on a representative Fe concentration in terrigenous matter [*Taylor and McLennan*, 1985] and the abundance of eolian matter in the cores [*Rea et al.*, 1986; *Chuey* et al., 1987]). This data indicates that the importance of dust storms, which can deposit Fe at a rate on the order of 3 mg cm^{-2} kyr^{-1} [*Young et al.*, 1991], may be underestimated by modern observations and that the average eolian estimates may not be representative of the longer scale input. With the recent observation that the EUC is an additional and important source of particulate Fe to the region [*Gordon et al.*, 1995], however, future research needs to quantify the amount of Fe from the EUC that is removed to the sediment (i.e., how much of the EUC Fe is indeed removed by particles settling

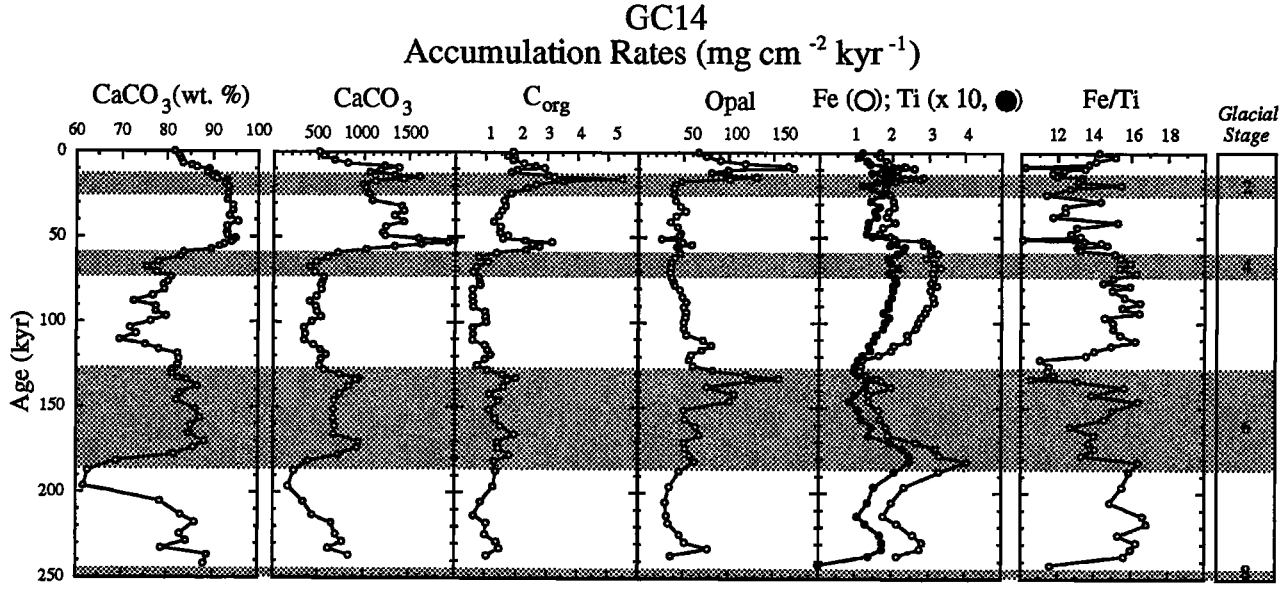

Figure 3. Downcore age profiles of the concentration of $CaCO_3$ (wt. %) in GC14 (with numbered and shaded isotopic glacial stages from *Imbrie et al.* [1984], note that glacial Stage 8 extends off the bottom of the figure), the accumulation rates of $CaCO_3$, C_{org}, opal, Fe, and Ti (x 10), as well as the age profile of Fe/Ti.

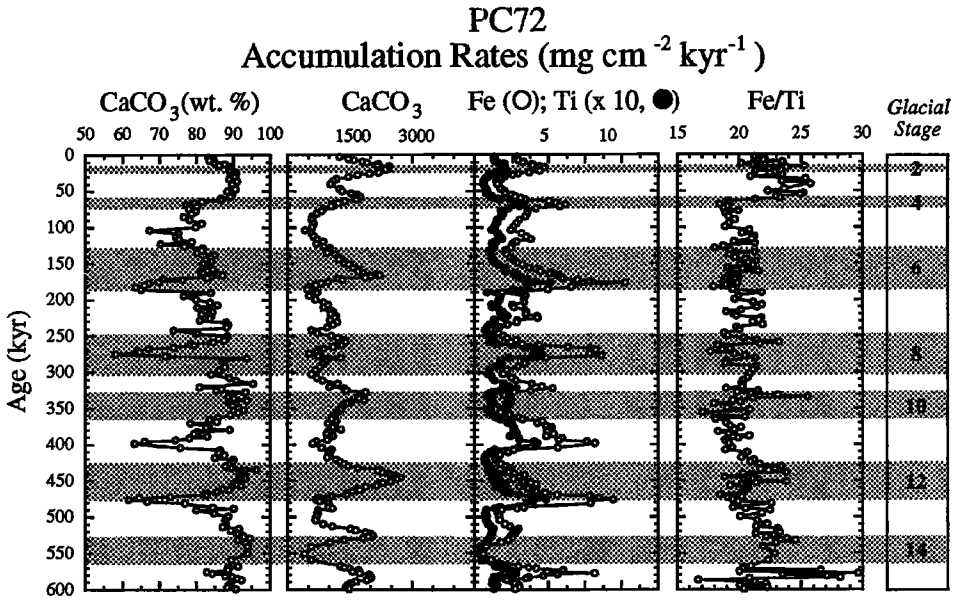

Figure 4. Downcore age profiles of the concentration of $CaCO_3$ (wt. %) in PC72 (with numbered and shaded isotopic glacial stages from *Imbrie et al.* [1984]), the accumulation rates of $CaCO_3$, C_{org}, opal, Fe, and Ti (x 10), as well as the age profile of Fe/Ti.

through the EUC). For example, previous studies of Fe and terrigenous deposition across the equatorial productivity gradient indicate that the flux of Fe and terrigenous material at ~ 4° N (located beneath the Intertropical Convergence Zone and intepreted as eolian in origin) is 3 to 5 times as large as the flux at the Equator [*Murray and Leinen*, 1993; *Murray et al.*, 1993]. This is also consistent with the fact that eolian fluxes are known to be larger in the northern hemisphere [*Duce and Tindale*, 1991]. Thus several issues relating to the particulate Fe cycle in the Central equatorial Pacific remain unresolved.

Conclusion

Chemical and mineralogic data from the equatorial Pacific indicate that there is no relationship between terrigenous input of Fe and burial of carbon on the glacial-interglacial timescale. We reiterate the following points:

1. The accumulation of terrigenous material in general, and terrigenous Fe in specific, shows no consistent glacial or interglacial maxima or minima.

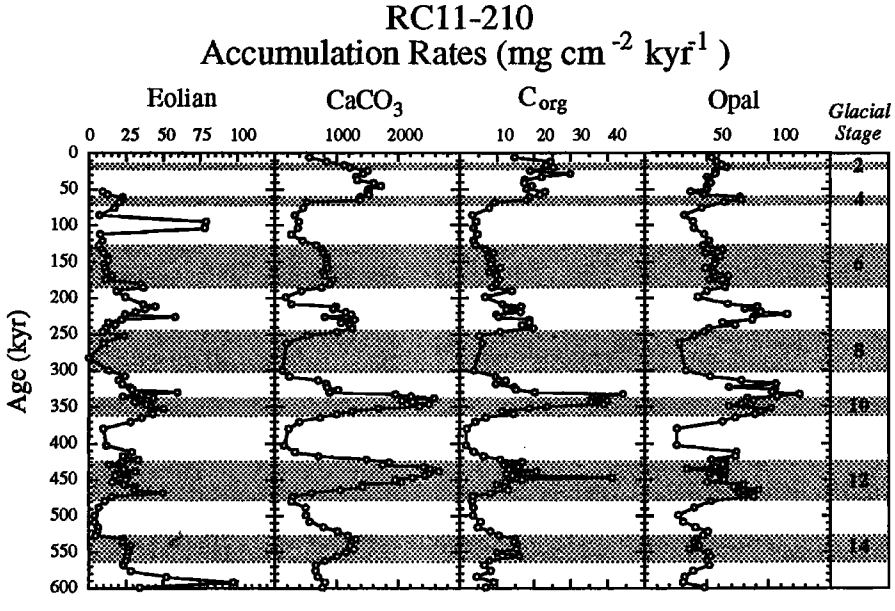

Figure 5. Downcore age profiles of the concentration of $CaCO_3$ (wt. %) in RC11-210 (with numbered and shaded isotopic glacial stages from *Imbrie et al.* [1984]), and of the accumulation rates of $CaCO_3$, C_{org}, and opal.

Table A1. Data for Core GC51

		weight %			mg cm^{-2} kyr^{-1}					
Depth, cm	Age, kyr	Fe	Opal	C_{org}	BAR	$CaCO_3$	Opal	C_{org}	Fe	Ti
0	0	0.28	16.9	0.47	845	615	143	3.97	2.25	0.106
5	3.75	0.21	15.8	0.16	1168	915	185	1.87	1.84	0.154
10	6.25	0.24	15.5	0.16	1348	1027	209	2.16	2.03	0.129
15	8.75	0.15	12.2	0.11	1477	1200	180	1.62	1.37	0.124
20	11.3	0.11	8.8	0.19	1528	1270	134	2.90	1.07	0.082
25	13.8	0.15	7.7	0.23	1385	1157	107	3.19	1.29	0.108
30	16.9	0.13	5.9	0.14	930	794	55	1.30	1.23	0.067
35	23.6	0.15	6.4	0.09	618	524	39	0.56	1.48	0.045
40	29.6	0.10	5.8	0.06	834	724	48	0.50	1.00	
45	33.8	0.09	5.7	0.06	957	836	54	0.57	0.86	0.040
50	38.3	0.11	6.4	0.06	910	792	58	0.55	1.02	
55	42.8	0.11	6.3	0.07	906	786	57	0.63	1.11	0.043
60	47.3	0.13	7.6	0.05	885	756	67	0.44	1.28	
65	51.8	0.11	5.6	0.06	840	734	47	0.50	0.97	0.035
70	57.1	0.11	6.7	0.05	772	677	52	0.39	1.04	
75	62.5	0.19	7.3	0.07	537	450	39	0.38	1.80	0.055
80	73.3	0.48	12.3	0.08	314	232	39	0.25	2.72	0.074
85	83.1	0.67	15.5	0.12	283	191	44	0.34	2.93	0.103
90	93.8	0.89	20.6	0.17	254	144	52	0.43	2.80	0.131
95	102	0.65	18.5	0.10	381	248	70	0.38	2.28	0.128
100	109	0.80	23.9	0.12	387	214	93	0.46	2.21	0.174
105	114	0.83	25.8	0.13	380	208	98	0.49	2.20	0.185
110	121	0.57	25.1	0.09	435	263	109	0.39	1.75	0.138
115	126	0.33	19.7	0.09	496	346	98	0.45	1.41	0.095
120	133	0.25	19.3	0.07	587	427	113	0.41	1.22	0.077
125	137	0.22	15.5	0.08	813	620	126	0.65	1.30	0.088
130	141	0.12	14.8	0.07	1085	839	160	0.76	0.74	0.085
135	144	0.18	14.0	0.09	1112	880	155	1.00	1.08	0.120
140	148	0.18	13.9	0.07	653	506	91	0.46	1.04	0.074
145	156	0.24	15.7	0.14	377	288	59	0.53	1.37	0.050
150	166	0.28	14.6	0.13	352	270	51	0.46	1.61	0.046
155	175	0.34	17.5	0.18	393	287	69	0.71	1.99	0.068
160	183	0.35	12.4	0.08	541	414	67	0.43	2.09	0.084
165	188	0.63	15.7	0.13	549	374	86	0.71	2.44	0.188
170	193	0.87	22.0	0.24	591	318	130	1.42	2.30	0.280
175	196	0.87	22.9	0.21	463	257	106	0.97	2.93	0.230
180	211	0.57	18.3	0.09	207	141	38	0.19	2.62	0.061
185	225	0.54	17.7	0.08	258	172	46	0.21	2.50	0.074
190	234	0.46	15.8	0.11	398	283	63	0.44	2.35	0.088
195	241	0.25	10.6	0.05	564	448	60	0.28	1.46	0.068
200	247	0.20	12.1	0.05	581	466	70	0.29	1.19	0.049
205	253	0.17	9.8	0.07	638	523	63	0.45	0.75	0.057
210	259	0.38	14.4	0.08	500	374	72	0.40	1.23	0.102
215	267	0.91	26.9	0.14	207	106	56	0.29	1.70	0.111
220	281	1.06	26.1	0.22	151	76	39	0.33	1.84	0.092
225	296	0.73	25.1	0.19	175	94	44	0.33	1.31	0.083
230	307	0.95	27.3	0.34	190	90	52	0.65	1.72	0.115
235	317	0.68	17.9	0.12	272	174	49	0.33	1.74	0.104
240	327	0.62	17.2	0.12	520	343	90	0.62	2.28	0.187
245	331	0.62	17.8	0.09	1373	881	245	1.24	5.34	0.494
250	332	0.22	12.7	0.05	2488	1961	317	1.24	2.48	0.298
255	334	0.15	7.7	0.05	2618	2218	201	1.31	1.92	0.173
260	335	0.12	6.9	0.04	2669	2290	183	1.07	1.65	
265	337	0.11	7.9	0.06	2654	2268	209	1.59	1.85	0.223
270	338	0.10	6.7	0.05	2705	2341	182	1.35	1.51	0.162
275	340	0.19	6.5	0.05	1825	1556	118	0.91	2.69	0.175
280	344	0.41	10.0	0.06	614	484	61	0.37	3.58	0.111
285	354	0.54	12.4	0.09	290	209	36	0.26	2.92	0.084

Table A1. (continued)

		weight %			mg cm^{-2} kyr^{-1}					
Depth, cm	Age, kyr	Fe	Opal	C_{org}	BAR	$CaCO_3$	Opal	C_{org}	Fe	Ti
290	365	0.64	13.0	0.12	264	185	34	0.32	2.64	0.098
295	377	0.62	13.0	0.12	267	198	35	0.32	2.40	0.088
300	389	0.79	15.5	0.09	234	147	36	0.21	2.29	0.101
305	400	0.81	17.2	0.15	248	151	43	0.37	2.16	0.110
310	410	0.82	18.4	0.11	256	155	47	0.28	2.15	0.115
315	420	0.14	6.9	0.04	704	606	48	0.28	1.01	0.038
320	424	0.17	6.8	0.04	910	786	62	0.36	1.32	0.044
325	429	0.07	4.3	0.04	974	879	42	0.39	0.65	0.047
330	433	0.15	3.5	0.03	975	880	34	0.29	1.35	
335	438	0.17	4.4	0.05	945	837	42	0.47	1.61	
340	442	0.07	3.5	0.05	1077	968	38	0.54	0.77	
345	446	0.12	3.3	0.04	952	846	32	0.38	1.15	0.040
350	451	0.14	4.6	0.04	937	825	43	0.37	1.40	0.051
355	455	0.19	4.9	0.04	1029	899	51	0.41	1.92	0.080
360	459	0.21	5.6	0.05	906	780	51	0.45	1.87	0.076
365	464	0.38	8.2	0.08	525	419	43	0.42	2.12	0.104
370	475	0.84	15.4	0.13	256	169	39	0.33	2.94	0.109
375	486	0.60	14.3	0.07	357	252	51	0.25	2.44	0.092
380	493	0.29	8.4	0.04	393	324	33	0.16	1.09	0.045
385	508	0.20	8.7	0.04	287	238	25	0.11	0.70	0.028
390	520	0.17	9.0	0.03	339	288	31	0.10	0.59	0.022
395	532	0.10	6.8	0.03	628	553	42	0.19	0.63	0.023
400	536	0.09	5.3	0.03	901	796	48	0.27	0.67	0.049
405	541	0.17	8.0	0.04	834	704	67	0.33	1.29	0.045
410	546	0.17	5.6	0.03	718	633	40	0.22	1.15	0.039
415	553	0.14	5.0	0.03	540	470	27	0.16	0.83	0.029
420	561	0.33	6.7	0.05	509	425	34	0.25	1.77	0.067
425	568	0.50	12.3	0.06	360	272	44	0.22	1.87	0.078
430	580	0.28	9.8	0.05	310	252	30	0.16	1.03	0.037
435	592	0.30	10.0	0.05	364	296	36	0.18	1.16	0.046
440	601	0.30	10.6	0.06	400	316	42	0.24	1.15	0.060
445	610	0.30	11.8	0.04	581	452	69	0.23	1.70	0.056
450	615	0.20	9.7	0.07	868	732	84	0.61	1.50	0.047
455	619	0.14	5.6	0.03	703	607	39	0.21	0.92	

Data for $CaCO_3$ wt. % and Ti wt. % are in *Murray et al.* [1993]. Ages from 0 to 412 kyr from isotopic model in *LaMontagne* [1993]; from 412 to 619 kyr from carbonate model in *Murray et al.* [1993]. BAR is bulk accumulation rate. Missing values in Ti accumulation are where Ti < detection limit.

Table A2. Data for Core GC14

		weight %					mg cm^{-2} kyr^{-1}					
Depth, cm	Age, kyr	$CaCO_3$	Opal	C_{org}	Fe	Ti	BAR	$CaCO_3$	Opal	C_{org}	Fe	Ti
0.5	0	82	10.8	0.30	0.27	0.019	618	504	66	1.88	1.67	0.12
3.5	2.48	83	11.1	0.25	0.24	0.016	679	560	75	1.71	1.65	0.11
6.5	4.81	83	11.1	0.23	0.23	0.016	813	674	91	1.88	1.83	0.13
9.5	6.79	83	12.0	0.23	0.19	0.014	990	826	118	2.24	1.90	0.14
12.5	8.17	85	11.5	0.18	0.16	0.016	1441	1228	166	2.62	2.36	0.23
15.5	9.22	86	10.8	0.18	0.16	0.012	1601	1384	172	2.91	2.59	0.19
18.5	10.40	89	7.5	0.15	0.16	0.013	1326	1182	99	2.02	2.13	0.17
21.5	12.07	89	6.7	0.15	0.14	0.012	1203	1067	81	1.83	1.69	0.14
24.5	13.59	91	6.8	0.21	0.14	0.012	1480	1340	100	3.03	2.13	0.18
27.5	14.67	90	7.3	0.18	0.16	0.012	1791	1611	131	3.22	2.86	0.21
30.5	15.74	91	6.4	0.35	0.17	0.013	1579	1434	101	5.45	2.73	0.21
33.5	17.10	93	3.9	0.29	0.17	0.013	1213	1129	48	3.50	2.07	0.16
36.5	18.97	93	3.8	0.25	0.17	0.011	1075	995	41	2.64	1.83	0.12
39.5	20.90	93	3.6	0.21	0.16	0.013	1093	1020	40	2.34	1.80	0.14

Table A2. (continued)

		weight %					mg cm^{-2} kyr^{-1}					
Depth, cm	Age, kyr	$CaCO_3$	Opal	C_{org}	Fe	Ti	BAR	$CaCO_3$	Opal	C_{org}	Fe	Ti
45.5	24.57	93	3.5	0.16	0.17	0.015	1132	1056	39	1.83	1.93	0.17
51.5	28.41	93	3.5	0.14	0.17	0.012	1177	1096	41	1.59	2.02	0.14
57.5	31.80	94	3.1	0.11	0.14	0.011	1501	1417	47	1.65	2.05	0.17
63.5	34.46	94	3.5	0.10	0.12	0.010	1526	1441	53	1.54	1.90	0.15
69.5	37.62	94	2.9	0.10	0.13	0.011	1431	1340	42	1.44	1.85	0.16
75.5	40.81	95	2.4	0.08	0.14	0.009	1509	1440	36	1.27	2.08	0.14
81.5	43.93	93	3.3	0.11	0.13	0.010	1330	1239	44	1.48	1.74	0.13
87.5	47.49	93	3.6	0.11	0.13	0.010	1299	1208	47	1.47	1.66	0.13
90.5	49.17	93	3.4	0.13	0.15	0.011	1327	1236	45	1.72	1.93	0.15
93.5	50.84	95	1.5	0.09	0.12	0.012	1685	1600	26	1.55	2.05	0.20
96.5	51.93	95	2.1	0.11	0.13	0.010	2108	1992	45	2.28	2.84	0.21
99.5	52.99	94	2.4	0.15	0.14	0.010	2042	1919	49	3.15	2.93	0.20
102.5	54.16	92	3.3	0.14	0.16	0.011	1761	1627	59	2.50	2.85	0.19
105.5	55.57	91	2.9	0.19	0.21	0.016	1465	1338	43	2.74	3.07	0.23
108.5	57.19	90	3.9	0.20	0.26	0.020	1151	1031	45	2.32	3.05	0.23
111.5	59.27	84	5.4	0.16	0.38	0.025	860	719	47	1.36	3.26	0.21
114.5	61.74	83	5.6	0.11	0.40	0.026	728	603	41	0.78	2.93	0.19
117.5	64.55	78	6.1	0.18	0.51	0.032	612	477	37	1.08	3.13	0.20
120.5	67.68	75	6.7	0.13	0.62	0.040	540	407	36	0.70	3.33	0.22
123.5	70.71	78	6.0	0.10	0.52	0.032	595	462	35	0.60	3.10	0.19
126.5	73.56	81	5.4	0.11	0.45	0.030	692	560	37	0.78	3.13	0.21
129.5	76.27	80	5.8	0.12	0.45	0.031	680	545	39	0.82	3.06	0.21
131.5	78.10	79	6.1	0.13	0.48	0.030	672	532	41	0.84	3.22	0.20
134.5	80.86	79	6.8	0.09	0.45	0.030	675	535	46	0.58	3.04	0.20
138.5	84.61	77	7.9	0.09	0.50	0.032	622	477	49	0.58	3.12	0.20
141.5	87.80	73	9.5	0.11	0.56	0.034	560	407	53	0.59	3.14	0.19
144.5	90.97	77	8.3	0.10	0.48	0.031	613	474	51	0.60	2.95	0.19
147.5	93.85	77	8.5	0.16	0.46	0.028	628	486	53	0.98	2.89	0.18
150.5	96.65	80	8.0	0.15	0.42	0.029	661	526	53	1.00	2.79	0.19
153.5	99.67	76	8.9	0.18	0.48	0.032	564	430	50	1.02	2.71	0.18
156.5	103.2	72	10.6	0.12	0.56	0.037	474	340	50	0.58	2.64	0.18
159.5	106.9	73	11.0	0.13	0.49	0.032	490	359	54	0.61	2.42	0.16
162.5	110.5	70	14.5	0.12	0.49	0.030	499	347	72	0.58	2.43	0.15
165.5	113.5	75	13.6	0.17	0.34	0.023	596	448	81	0.99	2.05	0.14
168.5	116.2	78	10.5	0.16	0.29	0.021	667	522	70	1.07	1.96	0.14
171.5	118.9	82	8.3	0.17	0.23	0.017	708	583	59	1.18	1.63	0.12
174.5	121.7	83	8.8	0.16	0.19	0.017	639	527	56	0.99	1.20	0.11
177.5	125.2	82	9.8	0.12	0.19	0.016	622	513	61	0.74	1.15	0.10
180.5	128.1	81	11.9	0.16	0.16	0.014	693	562	83	1.07	1.11	0.10
183.5	130.5	81	13.0	0.17	0.14	0.012	912	740	119	1.56	1.29	0.11
187.5	132.9	82	13.5	0.17	0.14	0.013	1155	952	156	1.99	1.59	0.15
189.5	134.0	84	11.6	0.16	0.16	0.012	1090	917	126	1.72	1.71	0.13
195.5	137.8	87	7.8	0.17	0.20	0.013	969	839	76	1.60	1.97	0.13
201.5	142.1	83	11.9	0.13	0.15	0.011	894	740	106	1.14	1.37	0.10
207.5	146.1	82	12.3	0.17	0.16	0.010	825	677	101	1.42	1.35	0.08
213.5	151.2	86	6.5	0.15	0.21	0.014	779	671	50	1.14	1.64	0.11
219.5	156.4	87	6.8	0.17	0.22	0.015	766	668	52	1.32	1.67	0.11
225.5	161.0	85	7.9	0.18	0.23	0.018	802	683	64	1.48	1.83	0.14
231.5	165.8	85	8.5	0.24	0.24	0.017	795	673	68	1.93	1.89	0.14
237.5	170.3	88	4.8	0.13	0.25	0.018	1075	948	51	1.41	2.65	0.19
243.5	173.8	86	4.8	0.13	0.30	0.021	1084	929	52	1.44	3.20	0.23
249.5	177.9	81	6.5	0.20	0.37	0.028	883	720	57	1.79	3.29	0.25
254.5	181.7	69	10.9	0.23	0.71	0.043	574	395	62	1.30	4.05	0.25
261.5	187.5	63	12.3	0.36	0.89	0.056	368	231	45	1.34	3.28	0.21
267.5	196.4	62	13.0	0.47	0.87	0.056	269	166	35	1.27	2.34	0.15
273.5	205.3	78	7.0	0.20	0.46	0.031	431	338	30	0.86	1.99	0.13
279.5	213.2	83	6.0	0.12	0.33	0.020	528	438	32	0.62	1.76	0.11
283.5	217.9	86	4.5	0.14	0.29	0.017	747	643	34	1.04	2.14	0.13
291.5	224.6	83	5.5	0.12	0.31	0.020	838	694	46	1.00	2.57	0.17
297.5	228.8	84	5.7	0.15	0.31	0.019	911	767	52	1.37	2.82	0.17
303.5	232.7	79	9.9	0.19	0.35	0.022	781	614	77	1.46	2.75	0.17
309.5	236.7	89	3.9	0.11	0.23	0.014	942	836	36	1.06	2.12	0.14

BAR is bulk accumulation rate.

Table A3. Data for Core PC72

Depth, cm	Age, kyr	BAR, mg cm^{-2} kyr^{-1}	$CaCO_3$, wt. %	Fe, ppm	Ti, ppm	mg cm^{-2} kyr^{-1} $CaCO_3$	mg cm^{-2} kyr^{-1} Fe	mg cm^{-2} kyr^{-1} Ti
15	2.74	1498	83.2	1514	71.2	1246	2.27	0.107
20	5.11	1751	83.9	1313	59.6	1469	2.30	0.104
25	7.20	1919	83.4	1212	55.2	1600	2.33	0.106
30	9.13	2127	84.8	1247	53.1	1804	2.65	0.113
35	10.92	2265	84.8	1144	54.0	1921	2.59	0.122
40	12.61	2494	87.5	1241	61.5	2182	3.10	0.153
45	14.23	2524	86.1	1247	59.1	2172	3.15	0.149
50	15.80	2734	89.3	1284	50.8	2442	3.51	0.139
55	17.35	2739	89.0	1380	58.0	2439	3.78	0.159
60	18.90	2722	89.2	1222	56.9	2427	3.33	0.155
65	20.48	2644	89.1	1268	56.6	2355	3.35	0.150
70	22.12	2516	88.9	1403	65.8	2237	3.53	0.165
75	23.85	2420	90.8	1219	53.2	2197	2.95	0.129
80	25.74	2187	90.6	1066	47.4	1981	2.33	0.104
85	27.86	1889	89.6	1074	45.7	1692	2.03	0.086
90	30.32	1631	90.3	948	45.3	1473	1.55	0.074
95	33.22	1337	88.8	1037	40.9	1187	1.39	0.055
100	36.62	1221	91.0	970	41.3	1111	1.18	0.050
105	40.30	1164	89.7	1067	41.4	1044	1.24	0.048
115	47.19	1390	90.6	1008	42.6	1259	1.40	0.059
120	50.15	1502	88.4	1050	47.0	1328	1.58	0.071
125	52.79	1722	89.8	948	37.6	1546	1.63	0.065
130	55.16	1880	89.7	1025	41.1	1685	1.93	0.077
135	57.37	1973	89.3	1095	47.6	1761	2.16	0.094
140	59.49	1929	86.7	1282	54.9	1672	2.47	0.106
145	61.60	1924	86.8	1435	67.3	1669	2.76	0.130
150	63.74	1704	81.5	2358	123.0	1389	4.02	0.210
155	66.05	1555	79.5	2832	147.2	1236	4.41	0.229
160	68.36	1385	77.3	3557	192.6	1070	4.93	0.267
165	70.96	1315	80.1	3508	184.1	1053	4.61	0.242
170	73.88	1124	77.9	2975	158.4	876	3.34	0.178
175	77.18	1030	79.8	2794	140.0	822	2.88	0.144
180	80.89	899	78.7	3173	167.5	707	2.85	0.150
185	85.03	783	76.6	3481	181.6	599	2.73	0.142
190	89.54	750	78.2	3217	163.7	586	2.41	0.123
195	94.30	767	81.4	2916	151.9	624	2.24	0.116
200	99.15	746	79.8	2748	145.5	595	2.05	0.109
205	103.88	623	67.3	3069	147.5	419	1.91	0.092
210	108.32	779	75.1	3228	159.3	584	2.51	0.124
215	112.37	850	74.5	3272	154.2	633	2.78	0.131
220	116.04	953	75.3	3187	151.8	717	3.04	0.145
225	119.37	1101	78.7	2026	103.4	866	2.23	0.114
230	122.4	999	70.3	2035	95.6	702	2.03	0.095
235	125.5	1147	76.7	1708	91.1	879	1.96	0.104
240	128.4	1254	81.8	1530	84.8	1025	1.92	0.106
245	131.4	1234	81.4	1361	70.6	1004	1.68	0.087
250	134.4	1211	80.2	1372	64.5	971	1.66	0.078
255	137.4	1360	85.0	1246	64.8	1156	1.69	0.088
263	141.8	1456	83.9	1285	65.3	1221	1.87	0.095
268	144.4	1508	84.1	1358	66.1	1243	2.05	0.100

Table A3. (continued)

Depth, cm	Age, kyr	BAR, mg cm^{-2} kyr^{-1}	$CaCO_3$, wt. %	Fe, ppm	Ti, ppm	mg cm^{-2} kyr^{-1} $CaCO_3$	mg cm^{-2} kyr^{-1} Fe	mg cm^{-2} kyr^{-1} Ti
273	146.8	1653	82.4	1336	62.3	1391	2.21	0.103
278	149.1	1677	84.2	1372	66.1	1373	2.30	0.111
283	151.3	1799	81.9	1433	71.3	1499	2.58	0.128
288	153.4		83.3	1596	75.6			
293	155.4	1915	82.9	1548	81.2	1588	2.97	0.156
298	157.4	2043	84.5	1625	80.0	1726	3.32	0.163
303	159.3	2082	83.1	1699	79.9	1730	3.54	0.166
308	161.0	2114	81.2	1692	78.5	1716	3.58	0.166
313	162.7	2230	81.7	1877	96.9	1821	4.19	0.216
318	164.4	2487	86.1	1629	83.5	2141	4.05	0.208
323	166.0	2555	87.0	1755	88.6	2223	4.48	0.226
328	167.6	2389	84.0	1916	97.4	2006	4.58	0.233
333	169.2	2263	83.0	2096	105.1	1878	4.74	0.238
338	171.0	1720	71.0	2762	146.3	1221	4.75	0.252
343	172.8	1745	76.2	3198	162.3	1329	5.58	0.283
348	174.9	1413	69.8	4399	234.2	986	6.22	0.331
353	177.1	1206	67.0	6792	341.9	808	8.19	0.412
358	179.6	1044	65.9	5194	274.4	688	5.42	0.286
363	182.5	863	63.5	6077	338.9	548	5.24	0.292
368	185.9	741	65.0	5349	274.2	481	3.96	0.203
373	190.0	854	83.9	1725	79.0	716	1.47	0.067
378	194.9	682	76.6	4013	200.8	522	2.74	0.137
383	199.6	847	79.9	3119	158.7	677	2.64	0.134
388	203.5	1040	83.8	2576	121.9	871	2.68	0.127
393	207.1	1143	85.8	1755	80.4	980	2.01	0.092
398	210.5	1084	80.3	1905	88.9	870	2.07	0.096
403	213.8	1217	83.7	2217	110.0	1018	2.70	0.134
406	216.9	1303	84.3	2131	112.4	1099	2.78	0.146
413	219.8	1290	81.3	2125	108.6	1049	2.74	0.140
418	222.6	1386	84.0	2416	122.3	1165	3.35	0.170
423	225.4	1370	83.4	2488	114.1	1142	3.41	0.156
429	228.2	1270	80.9	1781	82.5	1028	2.26	0.105
433	231.2	1353	88.0	1649	78.2	1190	2.23	0.106
438	234.4	1240	88.6	1392	63.6	1099	1.73	0.079
443	238.0	1091	88.2	1190	60.1	962	1.30	0.066
448	242.1	771	73.8	1472	73.5	570	1.14	0.057
453	246.2	893	80.3	1426	75.9	716	1.27	0.068
458	250.1	1192	88.3	1272	66.7	1053	1.52	0.080
463	253.3	1390	87.7	1240	61.0	1219	1.72	0.085
468	255.9	1573	87.5	1406	65.6	1377	2.21	0.103
473	258.5	1655	84.6	1152	49.6	1399	1.91	0.082
478	260.8	1573	78.3	1628	75.1	1232	2.56	0.118
483	263.0	1651	79.3	2125	116.2	1309	3.51	0.192
488	265.2	1498	73.8	3387	178.4	1105	5.07	0.267
493	267.3	1297	66.9	4811	249.7	868	6.24	0.324
498	269.6	1178	64.0	5607	300.6	754	6.60	0.354
503	272.0	1112	64.5	5670	320.0	718	6.31	0.356
508	274.5	911	58.2	6878	350.2	530	6.27	0.319
513	277.4	1041	71.6	6614	323.0	745	6.89	0.336
518	280.5	1371	93.8	2822	132.3	1285	3.87	0.181

Table A3. (continued)

Depth, cm	Age, kyr	BAR, mg cm^{-2} kyr^{-1}	$CaCO_3$, wt. %	Fe, ppm	Ti, ppm	mg cm^{-2} kyr^{-1} $CaCO_3$	mg cm^{-2} kyr^{-1} Fe	mg cm^{-2} kyr^{-1} Ti
523	284.1	1082	86.9	2466	129.8	940	2.67	0.140
528	288.1	979	87.4	2762	145.9	856	2.71	0.143
533	292.5	895	87.8	2608	122.4	786	2.34	0.110
538	297.4	788	86.2	2154	102.0	679	1.70	0.080
543	302.7	701	84.2	2181	104.6	590	1.53	0.073
548	308.2	807	89.1	2438	117.8	719	1.97	0.095
551	311.2	934	90.8	2360	115.9	848	2.20	0.108
558	315.6	1280	95.3	2421	119.9	1220	3.10	0.153
564	320.0	1260	80.9	2884	142.4	1019	3.63	0.179
568	322.7	1578	86.8	2674	141.1	1370	4.22	0.223
574	325.2	1669	85.3	1806	83.9	1425	3.02	0.140
578	327.5	2025	93.3	1034	52.1	1890	2.09	0.105
584	329.7	1970	89.9	896	42.7	1771	1.77	0.084
588	331.9	1974	89.4	796	34.4	1765	1.57	0.068
594	334.1	1933	88.7	981	38.4	1714	1.90	0.074
598	336.2	1938	90.3	985	46.7	1749	1.91	0.090
604	338.5	1974	93.8	921	47.2	1850	1.82	0.093
609	340.9	1719	89.1	1113	55.3	1531	1.91	0.095
614	343.5	1610	89.4	1165	64.7	1439	1.88	0.104
618	346.2	1502	89.8	1149	59.8	1349	1.73	0.090
624	349.2	1433	91.4	1126	59.1	1310	1.61	0.085
628	352.4	1391	92.8	1021	48.9	1291	1.42	0.068
634	355.7	1328	91.3	1046	61.2	1213	1.39	0.081
638	359.0	1301	89.3	1412	77.7	1161	1.84	0.101
644	362.2	1277	85.9	1841	89.9	1097	2.35	0.115
648	365.2	1283	83.7	2023	111.6	1074	2.60	0.143
654	368.2	1377	85.5	2671	140.9	1178	3.68	0.194
658	371.0	1245	78.5	2733	144.1	977	3.40	0.179
664	373.9	1365	83.3	2837	147.0	1137	3.87	0.201
668	376.7	1332	82.6	3118	154.7	1100	4.15	0.206
674	379.5	1459	89.0	2782	141.8	1299	4.06	0.207
678	382.5	1224	80.3	3204	175.1	983	3.92	0.214
684	385.5	1202	79.3	3563	185.8	953	4.28	0.223
688	388.4	1322	83.0	2942	141.4	1097	3.89	0.187
694	391.2	1287	78.2	3678	184.5	1006	4.73	0.237
698	393.8	1293	74.3	3529	186.7	961	4.56	0.241
702	395.9	1061	66.0	5733	302.8	700	6.09	0.321
708	398.6	975	63.3	6710	349.3	616	6.54	0.340
717	404.3	1086	75.7	4156	213.5	821	4.51	0.232
722	407.5	1236	86.4	1673	88.5	1068	2.07	0.109
727	410.9	1173	86.1	1513	73.3	1010	1.78	0.086
732	414.4	1177	87.7	1151	56.6	1032	1.36	0.067
737	417.9	1143	85.0	984	48.7	972	1.13	0.056
742	421.2	1313	90.0	863	40.7	1181	1.13	0.053
747	424.4	1426	89.7	907	43.4	1278	1.29	0.062
752	427.3	1543	88.9	904	41.8	1372	1.40	0.064
757	429.9	1670	87.8	989	42.3	1466	1.65	0.071
762	432.2	1898	89.6	974	44.4	1701	1.85	0.084
767	434.4	2311	96.3	828	38.1	2225	1.91	0.088

Table A3. (continued)

Depth, cm	Age, kyr	BAR, mg cm^{-2} kyr^{-1}	$CaCO_3$, wt. %	Fe, ppm	Ti, ppm	mg cm^{-2} kyr^{-1} $CaCO_3$	mg cm^{-2} kyr^{-1} Fe	mg cm^{-2} kyr^{-1} Ti
772	436.4	2354	93.0	716	32.0	2189	1.69	0.075
777	438.3	2481	92.2	734	30.8	2286	1.82	0.076
782	440.0	2632	92.5	799	39.4	2434	2.10	0.104
787	441.7	2704	91.7	994	47.1	2479	2.69	0.127
792	443.3	2796				2570		
797	444.9	2850	92.0	838	44.5	2622	2.39	0.127
802	446.4	2923	93.2	720	34.7	2723	2.11	0.102
806	447.7	2853	92.0	719	34.1	2625	2.05	0.097
812	449.6	2767	91.5	924	42.8	2532	2.56	0.118
817	451.2	2701	91.9	970	40.6	2482	2.62	0.110
822	452.9	2531	90.7	1196	56.0	2295	3.03	0.142
827	454.6	2410	90.8	1374	67.9	2189	3.31	0.164
832	456.5	2330	92.2	1051	54.4	2148	2.45	0.127
837	458.5	2115	89.7	1116	53.9	1897	2.36	0.114
842	460.6	1941	87.2	1484	71.9	1692	2.88	0.140
847	462.7	1956	88.9	1683	82.1	1739	3.29	0.161
852	464.9	1832	85.5	1820	89.6	1567	3.33	0.164
857	467.0	1748	82.6	2181	108.0	1443	3.81	0.189
862	469.2	1756	82.7	2536	137.3	1452	4.45	0.241
867	471.4	1466	72.9	4256	210.5	1069	6.24	0.309
872	473.6	1235	64.5	5467	286.3	797	6.75	0.354
877	475.8	1131	61.7	6663	341.7	698	7.54	0.387
882	478.2	1169	66.7	5426	272.0	779	6.34	0.318
887	480.7	1299	76.9	4860	214.9	999	6.32	0.279
892	486.6	1179	84.5	2232	114.3	996	2.63	0.135
897	488.3	1203	90.1	1879	91.5	1084	2.26	0.110
902	490.1	933	80.0	1547	68.8	746	1.44	0.064
907	494.4	860	84.9	1477	67.7	730	1.27	0.058
912	499.3	799	88.7	1645	81.8	708	1.31	0.065
917	504.4	787	87.9	1724	80.2	691	1.36	0.063
922	509.5	982	88.0	1629	73.2	864	1.60	0.072
927	513.2	1256	87.2	1479	69.2	1094	1.86	0.087
932	516.1	1668	91.5	1394	60.2	1526	2.33	0.100
937	518.6	1854	89.3	1195	51.7	1657	2.22	0.096
942	520.8	2080	90.8	1050	45.1	1889	2.18	0.094
947	522.8	2183	91.3	937	43.9	1994	2.05	0.096
952	524.9	2214	92.5	890	39.1	2048	1.97	0.087
957	526.9	2108	92.8	905	40.8	1957	1.91	0.086
962	529.2	1933	94.5	1025	43.0	1827	1.98	0.083
967	531.8	1499	91.3	1193	48.6	1368	1.79	0.073
972	535.3	1108	93.4	1292	56.2	1035	1.43	0.062
977	540.7	622	93.8	1004	45.8	584	0.63	0.029
982	550.5	436	93.9	1045	45.7	410	0.46	0.020
987	559.0	664	89.5	1358	60.8	595	0.90	0.040
992	567.8	1405	91.3	1656	79.1	1282	2.33	0.111
997	569.5	1539	89.0	1892	92.3	1370	2.91	0.142
1002	571.3	1707	88.6	1951	96.1	1506	3.33	0.164
1008	573.4	1932	82.8	2481	93.4	1711	4.79	0.181
1013	575.5	1907	82.8	2053	102.6	1579	3.92	0.196
1018	577.4	2063	84.3	3156	106.4	1740	6.51	0.219
1023	579.3	2251	88.0	1993	84.7	1981	4.48	0.191

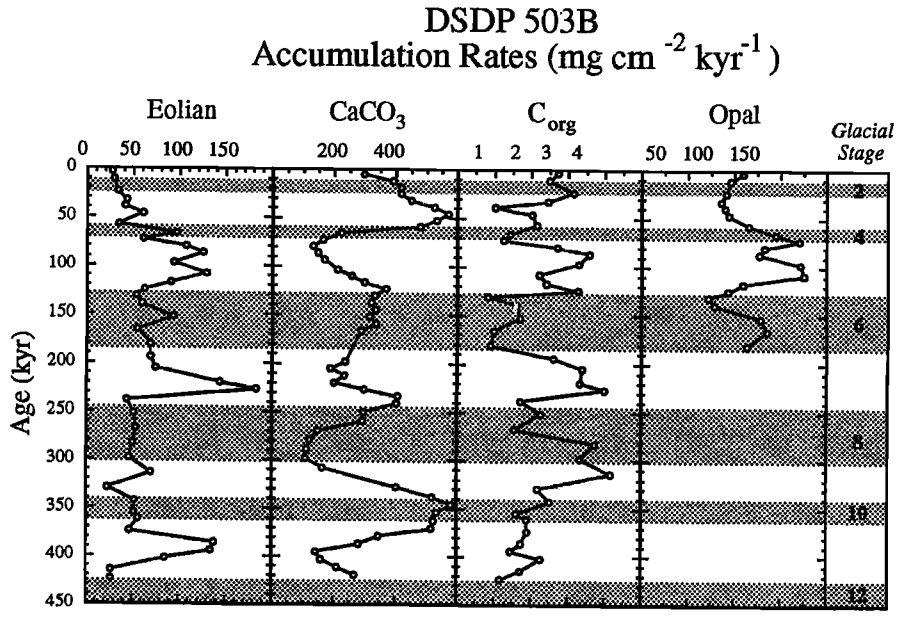

Figure 6. Downcore age profiles of the concentration of $CaCO_3$ (wt. %) in 503B (with numbered and shaded isotopic glacial stages from *Imbrie et al.* [1984]), and of the accumulation rates of $CaCO_3$, C_{org}, and opal.

2. The accumulation of the biogenic components $CaCO_3$, C_{org}, and opal show no linear r^2 or spectral relationship to that of terrigenous matter and Fe.

3. The linear r^2 and spectral correlations between Fe or eolian input and $CaCO_3$ concentration are either negative or zero and essentially 180° out-of-phase.

4. Collectively, therefore, there is no evidence that the input of Fe influenced the final sedimentary sequestering of biogenically produced carbon in the equatorial Pacific.

Thus while much biological and chemical oceanographic research has indicated that Fe may indeed serve as a micronutrient in surface waters (as cited above), the sedimentary record indicates that the terrigenous input of Fe is not implicated in glacial/interglacial cycles in productivity and biogenic accumulation. These combined data sets, in concert with previously published records from elsewhere around the globe (e.g., from ice cores), indicate that input of Fe and bulk particulate matter to surface waters is patchy both spatially and temporally. Future work should address the spatial and temporal scales of the patchiness, further target the potential for solubility variations in terrigenous source terrain, and focus on the importance of factors other than wind strength and aridity to the bulk transport of terrigenous material.

Appendix

Data for Core GC51 (Table A1), Core GC14 (Table A2), and Core PC72 (Table A3).

Table A3. (continued)

Depth, cm	Age, kyr	BAR, mg cm^{-2} kyr^{-1}	$CaCO_3$, wt. %	Fe, ppm	Ti, ppm	mg cm^{-2} kyr^{-1} $CaCO_3$	Fe	Ti
1028	581.1	2234	87.8	1659	61.2	1962	3.71	0.137
1033	583.0	2238	89.7	1304	46.3	2006	2.92	0.104
1038	585.0	2181	91.2	1254	60.2	1988	2.74	0.131
1043	587.0	2080	92.3	817	48.9	1920	1.70	0.102
1048	589.3	1846	89.6	1079	50.8	1654	1.99	0.094
1053	591.7	1729	89.3	1225	55.3	1543	2.12	0.096
1058	594.2	1649	88.8	1432	71.4	1464	2.36	0.118
1063	596.8	1610	88.4	1478	66.4	1423	2.38	0.107
1068	599.4	1650	90.8	1299	63.7	1497	2.14	0.105

BAR is bulk accumulation rate

Acknowledgments. Shipboard sample acquisition was funded by NSF grant OCE-8711221; shore based core curation, chemical analyses, and interpretation by NSF grants OCE-9022704, OCE-9022749, OCE-9102410, and OCE-930109. We thank F. Crease for helping sample Core PC72, P. M. Murray and D. Rea for comments on an earlier version of the manuscript, and Phil Howell at Brown University for assistance with the spectral analyses. Two anonymous reviewers provided helpful suggestions and clarifications. This is U.S. JGOFS contribution 203.

References

Archer, D., Equatorial Pacific calcite preservation cycles: Production or dissolution?, *Paleoceanography, 6,* 561-571, 1991.

Arrhenius, G. O. S., Sediment cores from the east Pacific, *Rep. Swed. Deep Sea Exped. 1947-1948, 5,* 1-228, 1952.

Barber, R. T., and F. P. Chavez, Regulation of primary productivity rate in the equatorial Pacific, *Limnol. Ocean., 36,* 1803-1815, 1991.

Berger, W. H., Deep-sea carbonates: Pleistocene dissolution cycles, *J. Foraminiferal Res., 3,* 187-195, 1973.

Berger, W. H., Pacific carbonate cycles revisited: Arguments for and against productivity control, in *Centenary of Japanese Micropaleontology*, edited by K. Ishizaki and T. Saito, pp. 15-25, Terra Scientific, Tokyo, 1992.

Berger, W. H., and G. Wefer, Productivity of the glacial ocean: Discussion of the iron hypothesis, *Limnol. Ocean., 36,* 1899-1918, 1991.

Boyle, E. A., Chemical accumulation variations under the Peru Current during the past 130,000 years, *J. Geophys. Res., 88,* 7667-7680, 1983.

Bruland, K. W., J. R. Donat, and D. A. Hutchins, Interactive influences of bioactive trace metals on biological production in oceanic waters, *Limnol. Ocean., 36,* 1555-1577, 1991.

Chuey, J. M., D. K. Rea, and N. G. Pisias, Late Pleistocene paleoclimatology of the Central Equatorial Pacific: A quantitative record of eolian and carbonate deposition, *Quat. Res., 28,* 323-339, 1987.

Condie, K. C., Chemical composition and evolution of the upper continental crust: Contrasting results from surface samples and shales, *Chem. Geol., 104,* 1-37, 1993.

DiTullio, G. R., D. A. Hutchins, and K. W. Bruland, Interaction of iron and major nutrients controls phytoplankton growth and species composition in the tropical North Pacific Ocean, *Limnol. Oceanogr., 38,* 495-508, 1993.

Duce, R. A., and N. W. Tindale, Atmospheric transport of iron and its deposition in the ocean, *Limnol. Oceanogr., 36,* 1715-1726, 1991.

Dymond, J., Geochemistry of Nazca plate surface sediments: An evaluation of hydrothermal, biogenic, detrital, and hydrogenous sources, in *Nazca Plate: Crustal Formation and Andean Convergence, Geol. Soc. Am. Memoir,* vol. 154, edited by L. D. Kulm, J. Dymond, E. J., Dasch, and D. M. Hussong, pp. 133-173, Geol. Soc. of Am., Boulder, Colo., 1981.

Dymond, J., E. Suess, and M. Lyle, Barium in deep-sea sediment: A geochemical proxy for paleoproductivity, *Paleoceanography, 7,* 163-181, 1992.

Emerson, S., Organic carbon preservation in marine sediments, in *The Carbon Cycle and Atmospheric CO_2: Natural Variations Archean to Present, Geophys. Monogr. Ser.*, vol. 32, edited by E. T. Sundquist and W. S. Broecker, pp. 78-87, AGU, Washington, D. C., 1985.

Farrell, J. W., and W. L. Prell, Pacific $CaCO_3$ preservation and $\delta^{18}O$ since 4 Ma: Paleoceanic and paleoclimatic implications, *Paleoceanography, 6,* 485-498, 1991.

Frost, B. W., and N. C. Franzen, Grazing and iron limitation in the control of phytoplankton stock and nutrient concentration: a chemostat analogue of the Pacific equatorial upwelling zone, *Mar. Ecol. Prog. Ser., 83,* 291-303, 1992.

Gordon, R. M., K. H. Coale, and K. S. Johnson, Iron distributions in the equatorial Pacific: Implications for new production, *Deep Sea Res,* in press, 1995.

Herguera, J. C., and W. H. Berger, Paleoproductivity from benthic foraminifera abundance: Glacial to postglacial change in the west-equatorial Pacific, *Geology, 19,* 1173-1176, 1991.

Herguera, J. C., and W. H. Berger, Glacial to postglacial drop in productivity in the western equatorial Pacific: Mixing rate vs. nutrient concentrations, *Geology, 22,* 629-632, 1994.

Hovan, S. A., D. K. Rea, and N. G. Pisias, Late Pleistocene continental climate and oceanic variability recorded in northwest Pacific sediments, *Paleoceanography, 6,* 349-370, 1991.

Imbrie, J., J. D. Hays, D. G. Martinson, A. McIntyre, A. C. Mix, J. J. Morley, N. G. Pisias, W. L. Prell, and N. J. Shackleton, The orbital theory of Pleistocene climate: Support from a revised chronology of the $\delta^{18}O$ record, in *Milankovitch and Climate, Part 1,* edited by A. L. Berger et al., pp. 269-305, D. Reidel, Norwell, Mass., 1984.

Jenkins, G. M., and D. G. Watts, *Spectral Analysis and Its Applications,* 525 pp., Holden-Day, Oakland, Calif., 1968.

Kolber, Z. S., R. T. Barber, K. H. Coale, S. E. Fitzwater, R. M. Greene, K. S. Johnson, S. Lindley, and P. G. Falkowski, Iron limitation of phytoplankton photosynthesis in the equatorial Pacific Ocean, *Nature, 371,* 145-149, 1994.

LaMontagne, R. W., A 400 k.y. record of preservation of calcite, opal and organic carbon in the central equatorial Pacific: Implications for paleo-CO_2 and late Pleistocene climate. MS thesis, Yale Univ., New Haven, Conn.. 1993.

Leinen, M., and D. Stakes, Metal accumulation rates in the central equatorial Pacific during Cenozoic time, *Geol. Soc. Am. Bull., 90,* 357-375, 1979.

Lyle, M., D. W. Murray, B. P. Finney, J. Dymond, J. M. Robbins, and K. Brooksforce, The record of late Pleistocene biogenic sedimentation in the eastern tropical Pacific Ocean, *Paleoceanography, 3,* 39-59, 1988.

Lyle, M. W., F. G. Prahl, and M. A. Sparrow, Upwelling and productivity changes inferred from a temperature record in the central equatorial Pacific, *Nature, 355,* 812-815, 1992.

Martin, J. H., Glacial-interglacial CO_2 change: the iron hypothesis, *Paleoceanography 5,* 1-13, 1990.

Martin, J. M., Iron as a limiting factor in oceanic productivity, in *Primary Productivity and Biogeochemical Cycles in the Sea,* edited by P. G. Falkowski and A. D. Woodhead, pp. 123-137, Plenum, New York, 1992.

Martin, J. H., S. E. Fitzwater, and R. M. Gordon, Iron deficiency limits phytoplankton growth in Antarctic waters, *Global Biogeochem. Cycles, 4,* 5-12, 1990.

Martin, J. H., R. M. Gordon, and S. E. Fitzwater, The case for iron, *Limnol. Ocean., 36,* 1793-1802, 1991.

Martin, J. H., et al., Testing the iron hypothesis in ecosystems of the equatorial Pacific Ocean, *Nature, 371,* 123-129, 1994.

Martin, W. R., M. Bender, M. Leinen, and J. Orchardo, Benthic organic carbon degradation and biogenic silica dissolution in the central equatorial Pacific, *Deep-Sea Res., 38,* 1481-1516, 1991.

Martinson, D., W. Menke, and P. Stoffa, An inverse approach to signal correlation, *J. geophys. Res., 87,* 4807-4818, 1982.

Morel, F. M. M., R. J. M. Hudson, and N. M. Price, Limitation of productivity by trace metals in the sea, *Limnol. Ocean., 36,* 1742-1755, 1991.

Murray, D. W., Spatial and temporal variations in sediment accumulation in the central tropical Pacific, Ph. D. dissertation, 343 pp., Oreg. State Univ., Corvallis, Oreg., 1987.

Murray, J. W., R. T. Barber, M. R. Roman, M. P. Bacon, and R. A. Feely, Physical and biological controls on carbon cycling in the equatorial Pacific, *Science, 266,* 58-65, 1994.

Murray, R. W., and M. Leinen, Chemical transport to the seafloor of the equatorial Pacific across a latitudinal transect at 135° W; Tracking sedimentary major, trace, and rare earth element fluxes at the Equator and the ITCZ, *Geochim. Cosmochim. Acta, 56,* 4141-4163, 1993.

Murray, R. W., M. Leinen, and A. R. Isern, Biogenic flux of Al to sediment in the Central equatorial Pacific Ocean: Evidence for increased productivity during glacial episodes, *Paleoceanography, 8,* 651-670, 1993.

Pedersen, T. F., Increased productivity in the eastern equatorial Pacific during the last glacial maximum (19,000 to 14,000 yr B. P.), *Geology, 11,* 16-19, 1983.

Pedersen, T. F., M. Pickering, J. S. Vogel, J. N. Southon, and D. E. Nelson, The response of benthic foraminifera to productivity cycles in the Eastern equatorial Pacific: Faunal and geochemical constraints on glacial bottom water oxygenation levels, *Paleoceanography, 3,* 157-168, 1988.

Pedersen, T. F., B. Nielsen, and M. Pickering, Timing of Late Quaternary productivity pulses in the Panama Basin and implications for atmospheric CO_2, *Paleoceanography, 6,* 657-677, 1991.

Peng, T. -H., and W. S. Broecker, Factors limiting the reduction of atmospheric CO_2 by iron fertilization, *Limnol. Oceanogr., 36,* 1919-1927, 1991.

Petit, J. R., L. Mounier, J. Jouzel, Y. S. Korotkevich, Y. I. Kotlayakov, and C. Lorius, Palaeoclimatological and chronological implications of the Vostok core dust record, *Nature, 343,* 56-58, 1990.

Pisias, N. G., and D. K. Rea, Late Pleistocene paleoclimatology of the Central equatorial Pacific: Sea surface response to the southeast trade winds, *Paleoceanography, 3,* 21-37, 1988.

Price, N., L. F. Andersen, and F. M. M. Morel, Iron and nitrogen nutrition of equatorial Pacific plankton, *Deep Sea Res., 38,* 1361-1378, 1991.

Rea, D. K., L. W. Chambers, J. M. Chuey, T. R. Janecek, M. Leinen, and N. G. Pisias, A 420,000-year record of cyclicity in oceanic and atmospheric processes from the eastern equatorial Pacific, *Paleoceanography, 1,* 577-586, 1986.

Rea, D. K., N. G. Pisias, and T. Newberry, Late Pleistocene paleoclimatology of the Central equatorial Pacific: Flux patterns of biogenic sediments, *Paleoceanography, 6,* 227-244, 1991.

Sarmiento, J. L., and J. C. Orr, Three-dimensional simulations of the impact of Southern Ocean nutrient depletion on atmospheric CO_2 and ocean chemistry, *Limnol. Oceanogr. 36,* 1928-1950, 1991.

Snoeckx, H., and D. K. Rea, Late Quaternary $CaCO_3$ stratigraphy of the eastern equatorial Pacific, *Paleoceanography, 9,* 341-351, 1994.

Taylor, S. R., and S. M. McLennan, *The Continental Crust: Its Composition and Evolution,* 312 pp., Blackwell, Cambridge, Mass., 1985.

Watson, A. J., C. S. Law, K. A. Van Scoy, F. J. Millero, W. Yao, G. E. Friederich, M. I. Liddicoat, R. H. Wanninkhof, R. T. Barber, and K. H. Coale, Minimal effect of iron fertilization on sea-surface carbon dioxide concentrations, *Nature, 371,* 143-145, 1994.

Wei, K. -Y, Z. -W. Zhang, M. -T. Chen, A. R. Isern, C. -H Wang, and M. Leinen, Late Quaternary paleoceanography of the Central Equatorial Pacific: A quantitative record of planktonic foraminiferal, isotopic, organic carbon and calcium carbonate changes, *J. Geol. Soc. China, 37,* 475-496, 1994.

Young, R. W., et al., Atmospheric iron inputs and primary productivity: Phytoplankton responses in the North Pacific, *Global Biogeochem. Cycles, 5,* 119-134, 1991.

C. W. Knowlton and M. Leinen, Graduate School of Oceanography, University of Rhode Island, Narragansett, RI 02882. (email:cknowlto@gsosun1.gso.uri.edu; mleinen@gsosun1.gso.uri.edu)

A. C. Mix, College of Oceanic and Atmospheric Sciences, Oregon State University, Corvallis, OR 97331. (email: mix@oce.orst.edu)

D. W. Murray, Department of Geological Sciences, Brown University, Providence RI 02912. (email: dmurray@brown.edu)

R. W. Murray, Department of Earth Sciences, Boston University, Boston, MA 02215 (email: rmurray@bu.edu)

(Received April 13, 1995; revised September 12, 1995; accepted September 20, 1995)